Journal of Geodesy manuscript No.
(will be inserted by the editor)

FG5's, offsets and drifts: Experience at Onsala Space Observatory from 2009–2018

Hans-Georg Scherneck · Marcin Rajner

Received: date / Accepted: date

Abstract At the end of the day we note that applying the Degree of Equivalence (DoE) to FG5 instruments at Onsala Space Observatory begs the question how reliable they are under transport—the FG5's and/or the DoE's). Analysis of almost 10 years of data from the Superconducting gravimeter (SG) there, has led us to the conclusion that the site has a low and manageable situation as far as environmental influences are concerned, and that the quantification of the SG's instrumental drift is precise enough to scrutinize and try identify points of weakness on the Absolute gravity (AG) side of the problem. Key to the method we apply is a full-scale reduction of all AG campaigns at our site using drop data and, instead of modelling external variation of gravity, use synchronized SG samples drawn from a low-pass filtered signal to reject distorted microseismic waveforms. We encounter drift in the AG's during setups, offsets far greater in size than the DoE's express, and seismic sensitivity, which we can cure thanks to drop data processing. It salvages one or the other campaign from being accounted with greater than necessary error bars. Before any reader puts this article aside at the notion that you cannot separate SG's instrumental drift from the real change of gravity, we have given the problem due attention and do think that absolute gravity can provide the required filter, but at the same time we rule out that FG5's are capable of reaching the accuracy required in studies of Glacial Isostatic Adjustment unless our generation trains its children's children to step into their fathers' trail. Instead, we hope, quantum gravimeters will soon make a difference.

Keywords Absolute gravimetry · Glacial Isostatic Adjustment · superconducting gravimeter · Onsala Space Observatory

H.-G. Scherneck
Chalmers University of Technology
Tel.: +46-31-7725556
E-mail: hgs@chalmers.se

M. Rajner
Warsaw University of Technology

1 Introduction

As laid out in Scherneck and Rajner (2019) (henceforth SR19) multi-campaign reduction at the drop level using a Superconducting gravimeter (SG) instead of a priori models for the temporal variation of gravity affords us a range of advantages in scrutinizing the performance of FG5 AG's. Drift during the AG setups can be discerned and the SG scale factor obtained more robustly, as Figure 1 demonstrates.

For the main points of this paper we shortly summarize the data and the methods employed to expose the major obstacles on the way toward an early, reasonably uncertain inference of the rate of change of gravity as an enterprise in a post glacial setting at large, and at Onsala Space Observatory (OSO), Sweden, in particular.

The primary reason for a secular change, a decrease of little-g, is attributed to Glacial Isostatic Adjustment (GIA). Models predict a value between -4.7 and -3.5 nm/s^2/yr at this site (Olsson et al. 2012, 2015, 2019). Being located near the coast of Kattegat, sea level change may play a though secondary role. Outrightly founded on crystalline bedrock, the influence of hydrology is much less there than at many other sites. We find a range of the admitted effect based on ECMWF's ERAin and ERA5 into the record of the SG (GWR OSG-054) at 4.0 nm/s^2/yr RMS and 22 nm/s^2/yr peak-to-peak range, which is on the order of the gravity residual in our most comprehensive variant of adjustment of tides and environmental parameters.

Concerning the SG, the samples we have obtained up to this date evaluate to 7,684,425,934 with only 335,666 lost (a 44 ppm leakage). Forming hourly ordinates and analysing for signals, the series is 74,204 hours long with 1,423 samples missing due breaks in SG operation, due to outlier rejection (criterion 4-σ and re-iteration), and as an inevitable consequence of the whitening filter as it widens data gaps.

The very fact that we arrive at a residual RMS this low is taken as vindication of a well achieved break-down of perturbing effects in terms of ancillary observations and models. Key enabling features are that

- the instrumental drift can be parametrized by a few jumps accompanied by changes in linear rate (four events), and two events followed by and exponential decay signature
- the stochastic noise can be approximated with a low-order Prediction-Error Filter (PEF, with less than ten coefficients).

Thus, a strategy to reduce the measurements of the 16 AG campaigns at OSO could be laid out which might appear as unorthodox as bold: All drop observations, 199,542 in total, are reduced using the SG data, its inferred drift function, and biases for AG-orientation (individually for each meter), an offset between the meters (after applying the results, the so-called Degrees of Equivalence (DoE) from International Comparison Campaigns, henceforth ICC), monument ties (OSO has four observation points); and secular drift rates for each setup of the AG's). The least-squares fit delivers also the scale

factor of the SG and the secular rate of gravity, the latter being afflicted by shortcomings in the cross-hair of this investigation. Table 1 shows campaigns, instruments, and drop yield.

In regard of references and citations concerning the analysis methods and strategies we refer to SR19. This article will devote itself to apply them to the specific case in the first hand, to discuss the matter in its own frame, and abstain from comparison with studies employing more orthodox methods at sites elsewhere. We think there is sufficient in content for the reader's take-away.

Two sources of systematic error are found to influence the secular rate of gravity change, (1) portability of the DoE's from the most recent ICC; (2) biases in the determination of the SG's drift, which conflates the instrumental with the geophysical, the AG's role being to disentangle them. The secular trend thus determined consists of everything not exhausted in the analysis of nine years of continuous SG measurements, i.e. not of atmospheric origin (we employ Atmacs in an advanced scheme) nor due to hydrology (ERA5) nor nontidal ocean loading (ECCO2) nor local "ocean" loading (using local tide gauges) nor leakage from (quasi-)periodic processes like Polar Motion. SR19 mention the lunar nodal tide as one of the more important sources of a rate bias owing to the need to extrapolate the body and loading tide response to its long period.

The strength of the use of unbroken SG data to jointly evaluate all AG campaigns is, besides the ability to search for trends during a setup, is that all environmental effects and the tidal variation of gravity can be considered equal as the AG platforms are at close range (the oft-visited AA and AC at only two metre).

1.1 SG scale factor

We don't consider the SG scale factor to change over time. There are good reasons, one being that the factor determined with quantum gravimeter GAIN (Freier et al. 2016) is almost compatible with the average of the set of FG5-campaigns; in those—second reason—setup slopes are not robust enough for estimation. If such slopes do occur in the AG, they regularly correlate with the tide signal, so that in our experience the spread of the scale factor over time is greater than the formal error (and the normalized error, unity χ^2/N, too). In order to shed light on a potentially hidden problem we investigated the residual of the multi-campaign adjustment, with setup slopes being adjusted, campaign by campaign (Figure 2). The individual campaigns resolve the scale factor with 0.4-5.2 nm/s^2/V uncertainty, while coefficients solved in the campaign-by-campaign inspection often make a close match. The results don't suggest a systematic variation of the SG's scale factor over time. However, what appears to happen in those cases where scale factors deviate is that significant setup slopes exist in those campaigns. Whence we propose that inferred variations of the scale factors reported in a range of studies may be biased due to setup slopes that were neglected, or better, are beyond what one can achieve when

campaigns are treated in isolation. When we said above "almost compatible" we admit that the two values differ more than their uncertainty. However, what will result from the discussion in section 3 is the sensitivity of the multi-campaign result to apparently significant excess meter offsets in some campaigns, so that suggesting GAIN v FG5 multi-campaign compatibility is still tentative at this point. Now, had setup slopes of the FG5X-220 during the GAIN campaign in Feb. 2015 been significant, the close fit achieved FG5: -774.83 ± 3.0, GAIN: -773.82 ± 0.21 nm/s^2/V lacks the crispiness of FG5 measurements in low microseismic noise conditions (the record breaking example being 201606a with the FG5-233 with only ± 0.32 nm/s^2/V uncertainty). This notion goes also for the detection of setup slopes in Feb.2016, so that the alleged close fit would not only be tentative too, but also weak in resolution.

The large signal that the residual co-variance analysis reaps from campaign 16 (red cross in Fig. 2) is worth further exploration for principle reason. So far we have approximated sagging AG behaviour with straight lines only. The lower-than-usual value of little-g obtained from this particular campaign is not low enough to explain a 35 nm/s^2/V difference, not by orders of magnitude, as it would imply a 4.5% lower sensitivity on the AG's part. It appears more plausible to search for higher order polynomials to describe AG-drift during the two setups; yet, it will be difficult to prove as it seems to be a rare condition.

1.2 Teleseismic perturbation, microseismoc noise

At the high end of the frequency scale, microseismic noise might cause high drop scatter. At the frequencies of teleseismic waves, the AG proved to be a reliable seismometer, only that the sampling rate is too low to be useful in seismology (see Fig. 3). Surprisingly, while motion at periodicities around 30 s is picked up by the FG5 with high fidelity including the positive sign of the response, the situation reverses in the microseismic band. With careful adjustment of the time-stamps issued by the FG5 control program, the maximum absolute value of cross-covariance between seismometer and FG5 implies a negative sign. In campaigns with an elevated microseismic noise level a significant part of the drop noise can be reduced as shown in Fig. 4. Thus, in the multi-campaign regression system the seismometer's acceleration series is subtracted from the AG drop sequence. Microseisms are blocked from invading the system via the SG series, owing to low-pass filtering (combined with the compensation of the GGP filter's group delay) as described in SR19.

In the nine years of operation two campaigns gained from applying this procedure: 201502a when the North Atlantic was in typical late-winter state of unrest, and 201806a when just bad luck had presented us of a 15 dB noise level upped above what's typical for a summer season. We have included this experience as it vindicates our method working with drop-stage data; it won't work on sets.

2 Results and discussion

The results from the multi-campaign analysis is given in Table 2. In the subsequent sub-sections aspects of our findings will be discussed.

2.1 Remarks on the uncertainty of rates and rate bias

The rate bias is a linear slope missing in the estimated drift function at the stage of SG data' tidal analysis. It originates in the set of environmental effects in regression. If any of these harbour a trend it is subtracted from the SG's drift with each of the respective series' admittance coefficient. This leakage is principally at work at all the signals in regression and trades slope signal with the drift terms. However, uncertainty in the sum of these terms arises only in the case of signals that contain stochastic errors; i.e. tides take no part in this. In order to calculate the rate bias uncertainty we need to quantify these stochastic components, which would multiply owing to each series' inherent difficulty. Along a more heuristic path we try to argue as follows: Assume the residual of the regression carries the spectral character of the modelling errors, probably dominated by the atmospheric model, itself conveying the largest gravity effect second only to the luni-solar tides. In Figure 6 the result of a Monte-Carlo exercise is shown. It starts with the estimation of a power spectrum using the MEM method to represent the residual. The prediction-error filter at the core of the method is applied inversely to generate 200 innovations of this noise. In principle drift-free by construction, fitting a straight line to the noise returns a set of non-zero rates, the histogram of which is used to determine the standard deviation of the slope rate. We find 0.2 nm/s^2/yr, which would be the upper bracket of the 1-σ range. More realistic values would scale with the fraction of signal (essentially: error) amplitude that the environmental series actually contribute. For the dominant term, Atmacs, the fraction is near 90%, so we choose to content ourselves with the uncertainty's face value of $\pm$0.2 nm/s^2/yr.

A rate bias in the secular trend could emerge for the reason that the offset related to meter orientation changes with the upgrades of the dropping chambers (from FG5 to FG5X). Notably, as we estimate instrument-specific orientation effects, they do turn out significantly different, see Table 2. However, Figure 7 does not fly systematic, urging evidence: the residuals of the two orientations flip from setup to setup in apparently unrelated sequence.

2.2 A problem of limited information

Concerning the rates of gravity change themselves, i.e. the SG drift term, a drawback in the current state of affairs arises due to the discontinuation of the ECCO2 ocean series. The plan to replace is by CMEMS, a Copernicus product, had to be dashed while problems with the reference system had to be fixed. In order to accommodate the AG campaign of 2018 the trends of the extended

SG analysis had to be extrapolated. Whence the subsequent chapter's efforts cannot be said other than being limited as of quantitative conclusions.

3 Assessment of campaign offsets

One set of parameters the authors have little hand on is yet worth considering as a target of inquiry, the ICC's. We devised a series of tests in which we add an incremental offset to each the official values and observe its impact on key parameters, which are the multi-campaign SG scale factor, the secular rate, and the residual RMS. The results of this exercise can be seen in Figure 5. The weighted averages of the unmodified residual, evaluated over each setup, is shown in Figure 7.

The quantities in the plot would provide a set of partial finite-differences from which a best fit solution could be constructed that yields a set of estimated campaign offsets. The danger to end up in a circle sporting nothing else but internal consistency led us to a more radical approach.

Turning the problem on its head we assume we know the secular rate from GIA modelling, (-3.6 nm/s^2/yr), apply the rate bias from SG analysis (-0.6 nm/s^2/yr), take the SG drift function at face value, use the scale factor of the SG from the GAIN campaign, and instead solve for campaign offsets along with the other parameters (orientation per instrument, platform ties, setup slopes. What we find (see Fig. 8) is a set that in shape is not unlike the DoE series but tends to exceed its amplitude, and that not only slightly. To blame this on the SG performance is a vain prospect, remembering the analysis with the simplest regression set (tides, local barometer and tide gauge) leaving us with less than 8 nm/s^2 RMS. The only place the SG residual has a conspicuous excursion of 20 nm/s^2 is in 201009a. Note, however, that the SG series has been subtracted from the AG right-off, and had the SG been offset for an instrumental reason, the extra offset of the FG5-233 with respect to the campaigns right before and after would have shown an inverted relation (the AG down if we had subtracted a false positive excursion). A drop downward of FG5X-233's offset in 2017 and continuing in 2018 has indeed been observed (A. Engfeldt, pers. comm.), but not to the extent we find.

At both ends of the time scale in Figure 8 the inferred offsets might of course be exaggerated due to the coerced secular term. But within a bound of all but implausible GIA rates, ± 3 nm/s^2/yr, the range of variation at the ends could not be more than 30 nm/s^2, i.e. dwarfed by the deviations that appear to persist throughout. As a test we imposed a secular term of zero (but kept the rate bias). The first and the second offsets changed by -25 nm/s^2, the last by $+7$ nm/s^2. For obvious reason the residual RMS of the fit did not change (as a single campaign wouldn't be sensitive to such a small secular rate).

The gain in residual RMS of the forced solution with respect to the one with the key parameters estimated is not spectacular: The normalized χ^2 decreases from 0.475 in the latter to 0.472. The numbers also tell us that the weights,

i.e. the error figures as stated in the drop files, are too large by a factor of 1.4 on average.

4 Conclusions

We used a simultaneous adjustment of all 16 Absolute gravity (AG) campaigns at Onsala Space Observatory, Sweden, since June 2009, by-passing a priori models of gravity variation and, instead, using a Superconducting gravimeter (SG). We extract its drift in a tide analysis with a range of time series in regression to account for non-tidal, environmental effects and a simple, quasi-deterministic function for the instrumental component of drift, and prediction-error filters to whiten the noise. The residual of the AG-SG adjustment indicates remanent offset during campaign far exceeding (by a factor of two) the Degrees of Equivalence determined in international comparison campaigns. The multi-campaign adjustment working with single drop measurements instead of normal-points (set averages) afforded us reduction of noise by employing a broadband seismometer in the cases of campaigns with elevated microseismic noise level. The efficiency of the FG5's "Super-spring" seemed limited; we propose that it over-compensates microseismic acceleration in the band with 2–10 s periods. At longer periods, the response to seismic surface waves ($\simeq$30 s) appeared almost undistorted.

The simultaneous adjustment of all setup facilitated the resolution of drifting behaviour, most probably on the part of the AG's. The low residual RMS of the multi-year SG analysis, order of 6 nm/s^2, argues against asserting that SG could episodically drift at order of 1 nm/s^2/h in typical setup durations of 12 h or more.

On the bottom line of this report stands the wish for future instrumental solutions in absolute gravimetry that are more robust as to varying mean levels, better isolated against ground vibrations, and capable for observing more samples, more tightly spaced over longer setups. Promising appears to be the concept of neutral atom interferometry.

References

Francis O, in total 48 authors (2013) The European Comparison of Absolute Gravimeters 2011 (ECAG-2011) in Walferdange, Luxembourg: results and recommendations. *Metrologia,* 50, 257–268,

Francis O, in total 45 authors (2015) International comparison of absolute gravimeters (ECAG-2013), CCM.G-K2 Key Comparison. *Metrologia,* 52, 07009, `https://doi-org.proxy.lib.chalmers.se/10.1088/0026-1394/52/1A/07009`

Freier C, Hauth M, Schkolnik V, Leykauf B, Schilling M, Wziontek H, Scherneck H-G, Müller J, Peters A (2016) Mobile quantum gravity sensor with unprecedented stability. *Journal of Physics: Conference Series,* 723:1, `http://stacks.iop.org/1742-6596/723/i=1/a=012050`,

Olsson P-A, Scherneck H-G, Ågren J (2012) Modelling of the GIA-induced surface gravity change over Fennoscandia. *J. Geodyn.,* 61, 12–22.

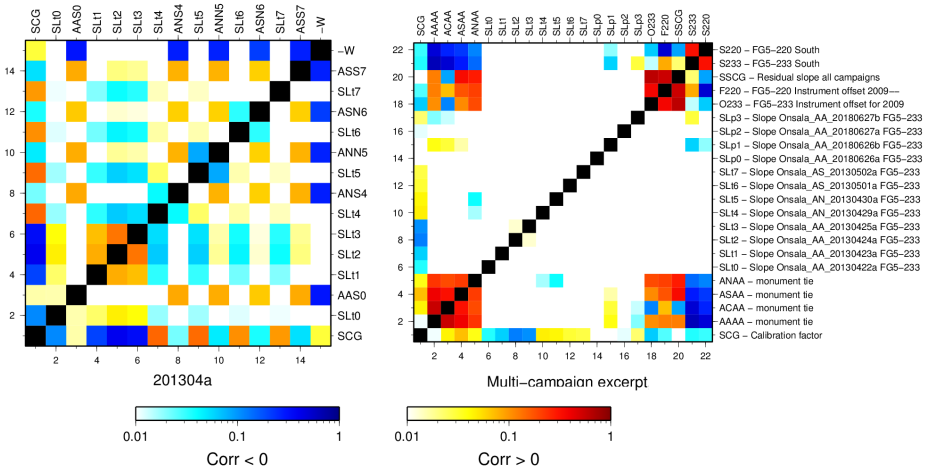

Fig. 1 - Parameter correlation in the multi-campaign adjustment compared with a single campaign (the one with greatest duration, 201304a, was chosen). In both cases setup slopes were estimated. Correlation inbetween monument ties turns out large regardless which; however, calibration factor and setup-slope parameters attain high correlation in the latter case, while the multi-campaign case gets much closer to orthogonality in general and on slope parameters in particular.

Table 1 Absolute gravity campaigns at Onsala Space Observatory from 2009 on, after the superconducting gravimeter had been installed.

No.	Campaign	Begin	End	Meter	ICC[a]	No.drops
1	200907a	2009-06-30	2009-07-07	FG5-233	10.0	8,890
2	200911a	2009-11-03	2009-11-06	FG5-220	17.0	7,850
3	201004a	2010-04-17	2010-04-21	FG5-220	17.0	5,509
4	201006a	2010-06-27	2010-07-02	FG5-233	47.0	6,239
5	201009a	2010-09-20	2010-09-23	FG5-233	47.0	2,626
6	201106a	2011-06-29	2011-07-04	FG5-233	22.0	4,800
7	201106b	2011-06-11	2011-06-17	FG5-220	11.0	14,249
8	201106c	2011-06-17	2011-06-19	FG5-220	11.0	2,400
9	201304a	2013-04-22	2013-05-03	FG5-233	22.0	16,791
10	201405a	2014-05-27	2014-06-02	FG5-233	25.3	25,839
11	201405b	2014-05-28	2014-05-31	FG5-220	52.0	4,594
—	201502g	2015-02-12	2015-02-25	GAIN		42,549[b]
12	201502b	2015-02-04	2015-02-12	FG5X-220	52.0	10,528
13	201505a	2015-05-06	2015-05-10	FG5-233	25.3	28,181
14	201606a	2016-06-27	2016-07-04	FG5-233	10.0	53,225
15	201707a	2017-07-05	2017-07-07	FG5X-233	10.0	8,200
16	201806a	2018-06-26	2018-06-27	FG5X-233	10.0	1,700

[a] nm/s^2
[b] samples starting Feb. 21; not part in multi-campaign adjustment

Olsson P-A, Milne GA, Scherneck H-G, Ågren J (2015) The relation between gravity rate of change and vertical displacement in previously glaciated areas. *J. Geodyn.*, 83, 76–84.

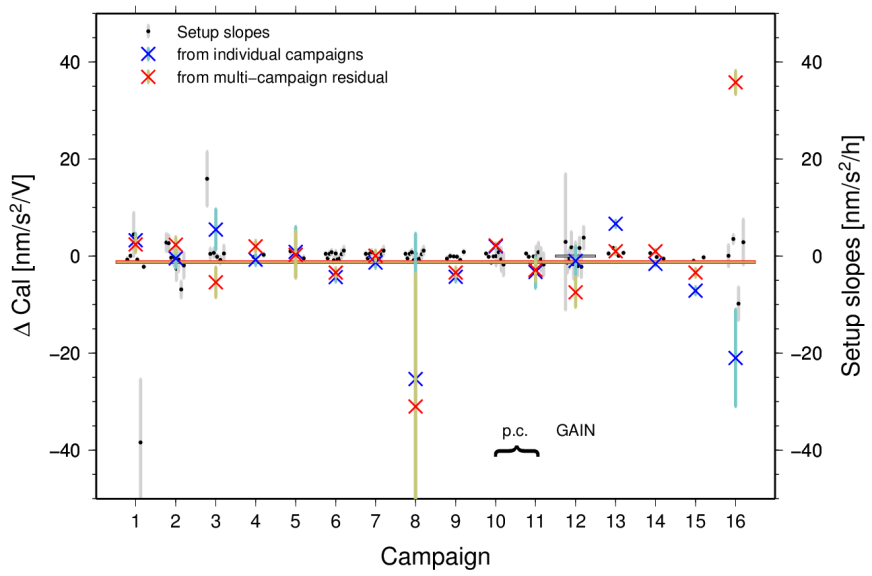

Fig. 2 AG setup slopes and SG scale factor and its residual signatures. The latter are determined from co-variation with the multi-campaign residual evaluated within the campaign subsets (red crosses). Also shown are scale factors determined from campaigns one at a time (blue crosses), then not reducing for setup slopes. There appears to be a relation between scale factor deviations and the presence of at least one significant setup slope in a campaign (most clearly at no.16, 201806a). The setup slopes are shown as small black dots and their error bars (standard deviation) in grey. The multi-campaign's solution for the scale factor is shown as the yellow horizontal line outlined by a red box to show its uncertainty. The value determined from the GAIN campaign in parallel to campaign no. 12 (201502b) is shown as a short horizontal grey bar (zero line), its thickness representing the uncertainty. Campaigns 10 and 11 in 2015 were conducted in parallel with the two FG5's (220 and 233, marked as p.c.).

Olsson P-A, Breili K, Ophaug V, Steffen H, Bilker-Koivula M, Nielsen E, Oja T, Timmen L (2019) Postglacial gravity change in Fennoscandia three decades of repeated absolute gravity observations. *Geophys. J. Int.,* ggz054, doi:/10.1093/gji/ggz054

Pálinkáš V, Francis O, Val'ko M, in total 37 authors (2017) Regional comparison of absolute gravimeters, EURAMET.M.G-K2 key comparison. *Metrologia, 54:1A*, 07012, `https://doi.org/10.1088/0026-1394/54/1A/07012`

Scherneck H-G, Rajner M (2019) Using a Superconducting Gravimeter in Support of Absolute Gravity Campaigning — A feasibility study *Geophysica*, 21pp, accepted, preprint at `https://eartharxiv.org/yxvjc/`

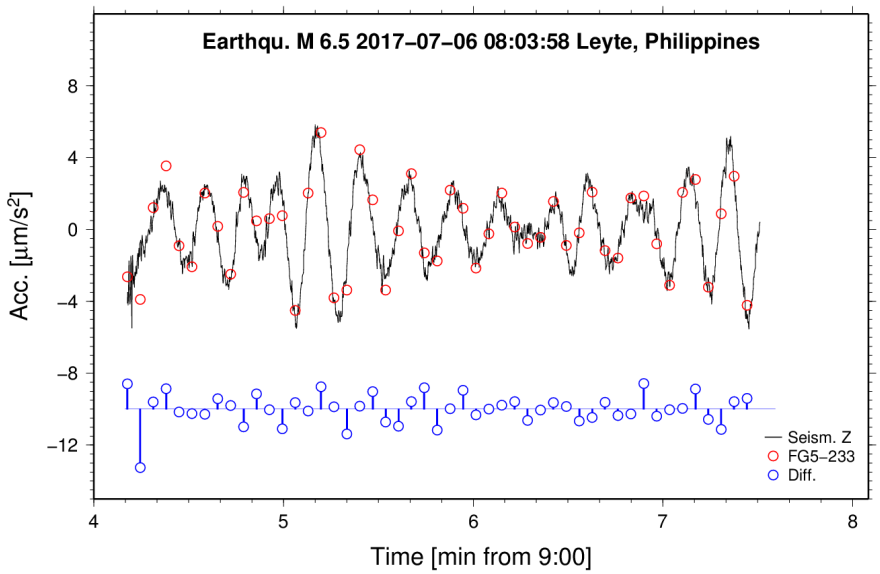

Fig. 3 Seismic surface wave train after an earthquake in the Philippines. The FG5X-233 picked up the vertical accelerations at 1 μm/s^2 RMS difference with respect to the broadband seismometer at Onsala, station ONA of the Swedish National Seismic Network. The seismometer's calibration factor had to be honed a little, and the time stamps of the AG series were adjusted to yield maximum correlation at zero lag, owing credit to the seismometer's GPS-controlled clock.

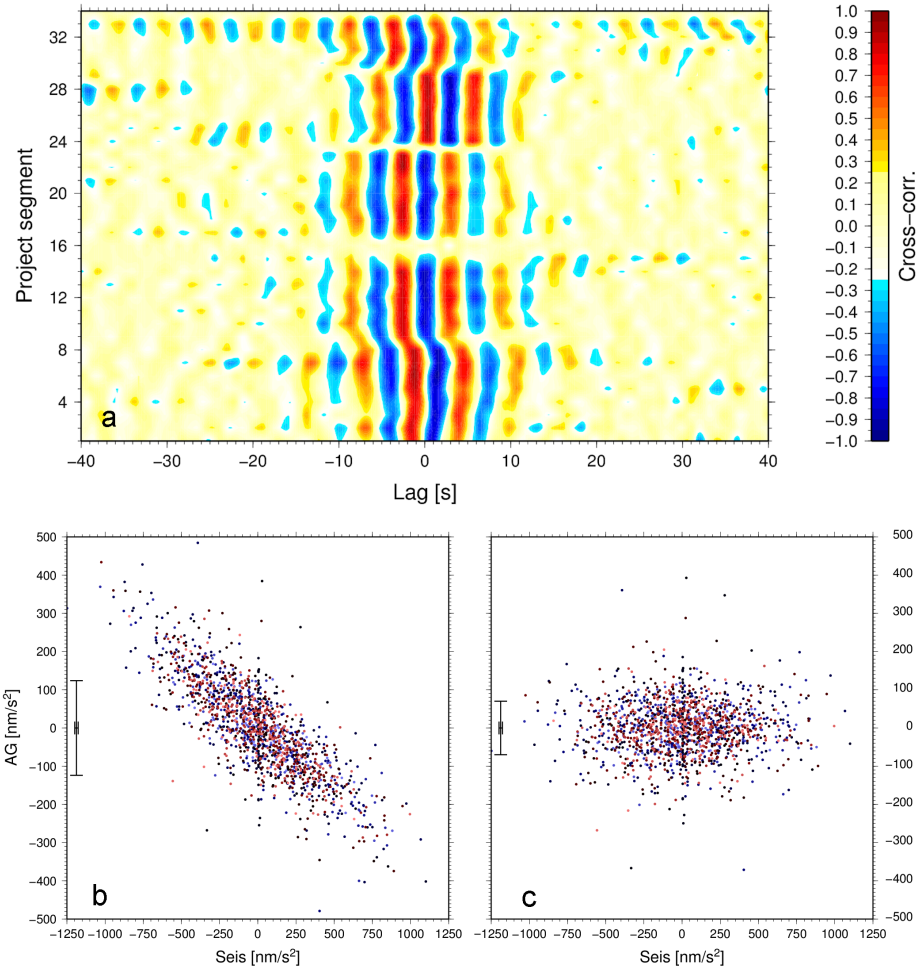

Fig. 4 Frame **a** shows the determination of AG time stamp corrections using the seismometer. The cross-covariance between the two instruments' time series has been calculated from two-hour segments (vertical axis). Frames **b** and **c** show a scatter plot before and after regression, respectively, determining a coefficient for each segment. The colour of the dots change from blue to red as campaign time passes along. Note that the correlation between acceleration measured with the AG and with the seismometer is negative. More on that in the main text. The reduced drop series loses 50% of its original RMS-scatter as indicated by the error bar's vertical line (the horizontal shows the repeatability of measuring seismometric acceleration).

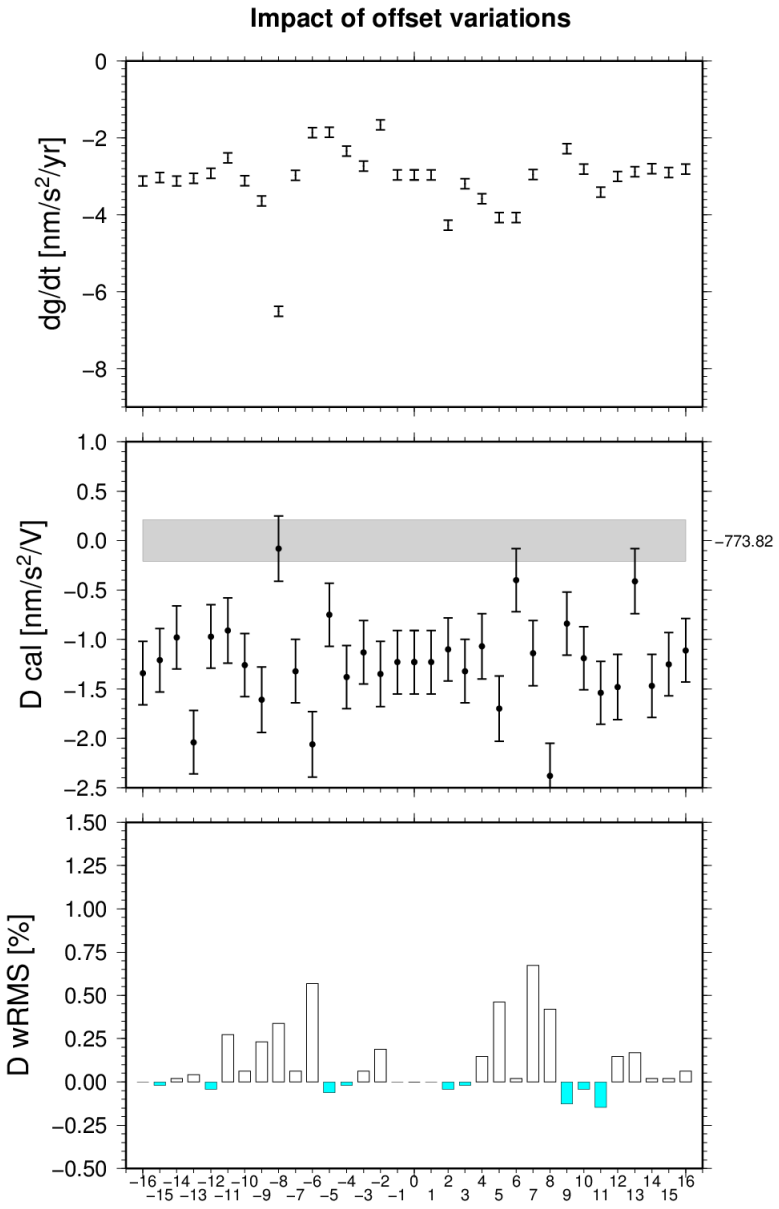

Fig. 5 Varying the DoE's from the ICC's by a typical AG uncertainty value (20 nm/s^2) in every one of the 16 campaigns once with a minus sign (left half of the abscissa), once with a plus (right), key parameters are affected, the secular rate (top frame), the SG's scale factor (mid; the scale factor in GAIN campaign −773.82 ±0.21 nm/s^2/V serving as a reference). The weighted RMS of the over-all fit (bottom). Of the 16 campaigns, those showing a lower RMS with offset increments added to the DoE's (coloured bars) are candidates for continued inspection.

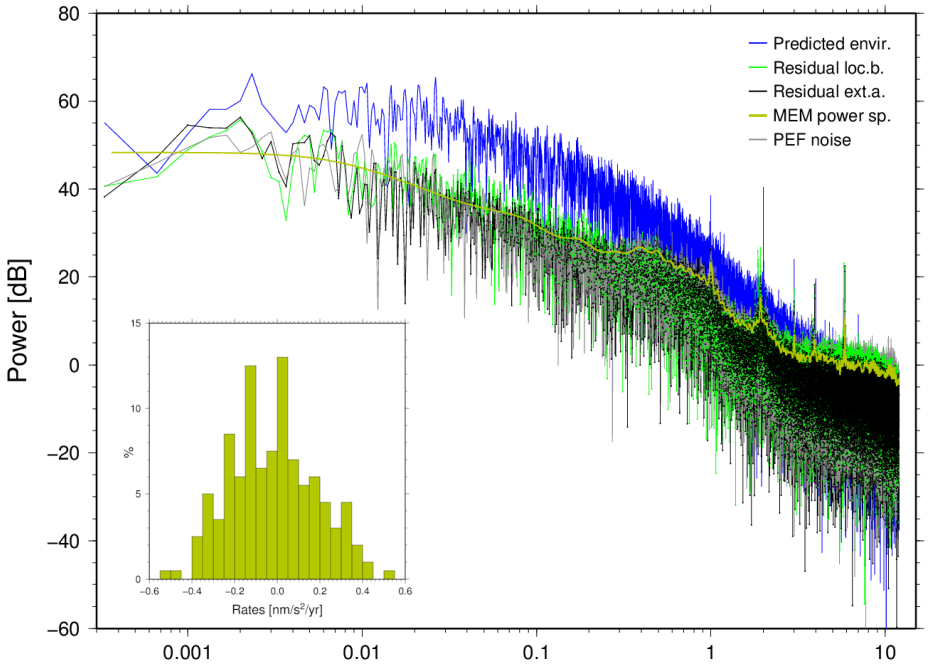

Fig. 6 Estimating the uncertainty of the rate bias. Shown are periodograms (unless indicated otherwise) for the reason that here important long-period end is unaccessible to windowed stacking methods like Bartlett's procedure. The spectrum of the sum of environmental effects determined in least-squares regression is shown in dark blue, the residual of the adjustment in the extended analysis in black, the residual where only the local barometer and the tide gauge are used (no hydrology, no non-tidal ocean loading) in green. The extended analysis' residual is modelled with a prediction-error filter of length 300 (using the MEM method of Burg), shown in yellow. With this filter and a random Gaussian deviate generator, 200 artificial series are produced in which linear trends are found. A histogram of the rates of these trends is shown in the inset. The spectrum of one of the artificial series is shown in grey. The MEM spectrum shown is yet unscaled; in the simulation the reproduction of the residual's RMS is duly warranted.

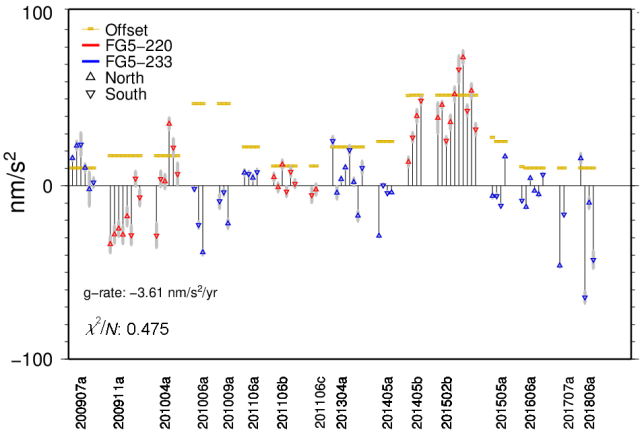

Fig. 7 Residual averaged over each setup. The official DoE's are applied (Francis et al. 2013, 2015; Pálinkáš et al. 2017). The secular rate of -3.61 nm/s^2/yr given in the diagram has an uncertainty of ± 0.32 nm/s^2/yr in the least-squares fit; the rate bias, however, adds ± 0.2 nm/s^2/yr to it.

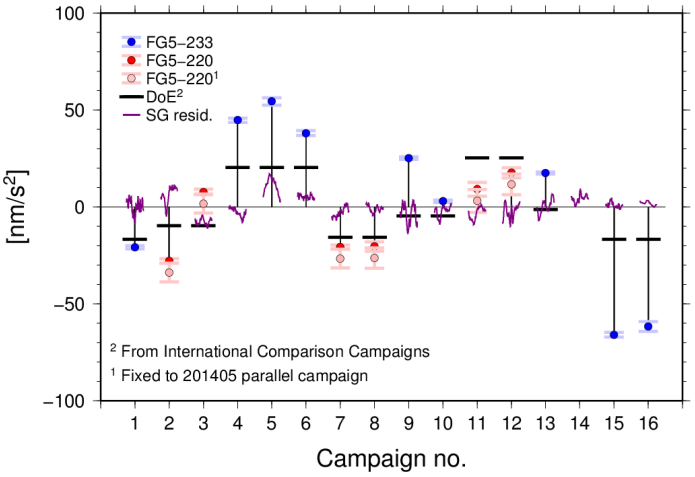

Fig. 8 Official DoE's and estimated campaign offsets assuming known key parameters: secular rate of gravity, SG scale factor, SG drift and rate bias. The SG's residual during the campaigns is shown in purple. In the account of FG5-220, the variant nailing the meters' differential offset to zero at the parallel campaign in 2015 is shown in pink, the unconstrained one in red.

Table 2 Results of multi-campaign adjustment. The SG drift function was not adjusted, only subtracted. Uncertainty is rescaled to yield a normalized χ^2 of the residual.

Symbol	*Parameter*	*Std.dev.*
Significant setup slopes [nm/s^2/h] [a]		
AS 20090702a	−0.73	0.33
AC 20090705a	−0.73	0.27
AC 20090706a	−38.42	13.00
AC 20090706b	−2.21	0.19
AA 20091105c	−6.88	1.70
AS 20100417a	15.96	5.60
AA 20100627a	−0.21	0.06
AN 20130429a	−0.82	0.35
AN 20130430a	0.86	0.36
AS 20130501a	0.99	0.47
AS 20130502a	1.15	0.35
AC 20140527a	0.51	0.10
AA 20140530a	−1.32	0.17
AA 20150506a	0.56	0.15
AA 20150507a	1.65	0.16
AC 20150509a	0.64	0.10
AC 20160627a	0.58	0.10
AA 20160629a	−0.56	0.15
AA 20170705a	−1.00	0.28
AA 20180626b	3.50	0.88
AA 20180627a	−9.77	3.40
Secular rate [nm/s^2/yr] [b]		
	−2.96	0.13
Meter offsets [nm/s^2]		
FG5-233	−54.47	1.07
FG5-220	−43.32	0.89
Offset orient south [nm/s^2]		
FG5-233	−33.09	0.53
FG5-220	−15.44	1.15
Scale factor [nm/s^2/V]		
OSG-054	−775.05	0.32
Monument ties [nm/s^2]		
AA	2.93	0.73
AC	62.49	0.51
AS	3247.03	0.89
AN	3159.94	1.35

[a] $|\dot{g}| > 2\sigma$
[b] rate bias not included